Available online at www.sciencedirect.com

SciVerse ScienceDirect

journal homepage: www.elsevier.com/locate/watres

Relation between EPS adherence, viscoelastic properties, and MBR operation: Biofouling study with QCM-D

Amer Sweity [a], *Wang Ying* [a], *Mohammed S. Ali-Shtayeh* [b], *Fei Yang* [a], *Amos Bick* [c], *Gideon Oron* [a], *Moshe Herzberg* [a,*]

[a] *Ben Gurion University of the Negev, Zuckerberg Institute for Water Research, Sede Boqer Campus, Midreshet Ben Gurion, 84990, Israel*
[b] *Biodiversity & Environmental Research Center (BERC), Til Village, P.O.BOX 696, Nablus, West Bank, Palestinian Authority*
[c] *Department of Industrial Engineering and Management, Jerusalem College of Technology, Jerusalem, Israel*

ARTICLE INFO

Article history:
Received 23 June 2011
Received in revised form
16 September 2011
Accepted 19 September 2011
Available online 29 September 2011

Keywords:
Biofouling
MBR
QCM-D
EPS
Ultrafiltration
Wastewater

ABSTRACT

Membrane fouling is one of the main constraints of the wide use of membrane bioreactor (MBR) technology. The biomass in MBR systems includes extracellular polymeric substances (EPS), metabolic products of active microbial secretion that adversely affect the membrane performance. Solids retention time (SRT) in the MBR is one of the most important parameters affecting membrane fouling in MBR systems, where fouling is minimized at optimal SRT. Among the operating parameters in MBR systems, SRT is known to strongly influence the ratio of proteins to polysaccharides in the EPS matrix. In this study, we have direct evidence for changes in EPS adherence and viscoelastic properties due to changes in the sludge removal rate that strongly correlate with the membrane fouling rate and EPS composition. EPS were extracted from a UF membrane in a hybrid growth MBR operated at sludge removal rates of 59, 35.4, 17.7, and 5.9 L day^{-1} (corresponding SRT of 3, 5, 10, and 30 days, respectively). The EPS adherence and adsorption kinetics were carried out in a quartz crystal microbalance with dissipation monitoring (QCM-D) technology in several adsorption measurements to a gold sensor coated with Polyvinylidene Fluoride (PVDF). EPS adsorption to the sensor surface is characterized by a decrease of the oscillation frequency and an increase in the dissipation energy of the sensor during parallel flow of aqueous media, supplemented with EPS, above the sensor surface. The results from these experiments were further modeled using the Voigt based model, in which the thickness, shear modulus, and shear viscosity values of the adsorbed EPS layers on the PVDF crystal were calculated. The observations in the QCM-D suggested that the elevated fouling of the UF membrane is due to higher adherence of the EPS as well as reduction in viscosity and elasticity of the EPS adsorbed layer and elevation of the EPS fluidity. These results corroborate with confocal laser scanning microscopy (CLSM) image analysis showing thicker EPS in close proximity to the membrane surface operated at reactor conditions which induced more fouling at elevated sludge removal rates.

* *Corresponding author*. Tel.: +972 8 6563520; fax: +972 8 6563503.
E-mail address: herzberg@bgu.ac.il (M. Herzberg).
0043-1354/$ – see front matter © 2011 Elsevier Ltd. All rights reserved.
doi:10.1016/j.watres.2011.09.038

1. Introduction

Membrane fouling is one of the main constraints of the wide use of membrane bioreactor (MBR) technology (Judd, 2006) causing an increase in the trans-membrane pressure (TMP) or a decrease in the permeate flux. During the biofouling process, membrane permeability decreases and energy consumption increases (Yang et al., 2006). Membrane fouling in MBR processes almost always consists of a combination of colloidal, organic, and microbial deposits (biofouling) as well as inorganic precipitates (scaling). These fouling factors increase the membrane hydraulic resistance over time and the permeate flux is consequently reduced. In most cases, deposition of the foulants are found both on the external membrane surface with some degree of foulant deposition inside the microfiltration (MF) and ultrafiltration (UF) membrane pores (Chang et al., 2002). Membrane biofouling is strongly related to membrane properties, operational conditions and biomass characteristics that include extracellular polymeric substances (EPS) properties. Hybrid growth MBR (HG-MBR) system can be defined as the combination of a membrane separation process and a hybrid growth processes, in which both suspended and attached-growth microorganisms are part of the MBR (Sombatsompop et al., 2006; Yang et al., 2006). HG-MBR allows for upgrading the treatment capacities of existing MBR treatment plants by increasing biomass level. Since both attached- and suspended-growth are involved, the HG-MBR can be operated at lower mixed liquor suspended solids (MLSS) concentrations. Membrane fouling is minimized without loss of the treatment efficiency due to biological activity of the microorganisms that are attached to the support carriers.

EPS, metabolic products of active bacterial secretion (Comte et al., 2006; Nuengjamnong et al., 2005), can be found either in a soluble form (also termed as soluble microbial products – SMP) or bound to cells or flocs in the reactor forming the cohesive matrix of the biofilms. Bound EPS consist of proteins, polysaccharides, nucleic acids and lipids accumulating on the bacterial cell surface (Morgan et al., 1990). The EPS strongly affect the microbial microenvironment heterogeneity including changes in porosity, density, water content, sorption properties, charge, hydrophobicity, and mechanical stability (Flemming and Wingender, 2001). One of the most effective MBR operating parameters with an impact on fouling propensity is solids retention time (SRT) or sludge age. SRT affects various sludge properties such as floc size, bound and soluble EPS content, and settling characteristics (Le-Clech et al., 2006).

Contradictory reports regarding a relationship between SRT and membrane biofouling show that even though higher SRT leads inevitably to increase of MLSS concentration, this in itself may not necessary lead to greater fouling. In general, optimal SRT, reported in plethora of studies between 20 and 50 days, is required to achieve a minimal fouling tendency (Meng et al., 2009; Drews, 2010; Kraume and Drews, 2010). Improved membrane permeability was observed at longer SRT of 10 and 20 days in comparison to SRT of 3 and 5 days. The results were attributed to elevated concentrations of SMP and EPS concentrations that were observed to induce membrane fouling rate when SRT was decreased (Ng et al., 2006). Cho et al. (2005a) showed that as SRT decreased, the amount of bound EPS in the sludge flocs increased (Cho et al., 2005b). Han et al. (2005) has reported that membrane fouling rate increased with increasing SRT of 30, 50, 70, and 100 days due to a large amount of foulants and high sludge viscosity (Han et al., 2005). In contrast, Lee et al. (2003) tested three lab-scale submerged MBRs at SRT of 20, 40, and 60 days with a constant permeate flux and no major change in EPS concentration was observed as SRT increased (Lee et al., 2003). In another study, at elevated MLSS concentrations from 7 to 18 g/l corresponding to an increase in SRT from 30 to 100 days, fouling rate was twice for the extended SRT (Al-Amoudi and Farooque, 2005). This increase was probably due to the raised viscosity at the high MLSS concentration that attenuates the effect of bubbling and scouring of the membrane surface. Not surprisingly, fouling rate increased nearly 10 times when SRT was lowered from 10 to 2 days, probably due to the increased levels of EPS production (Trussell et al., 2006).Chang and Lee (1998) found that when the SRT was increased from 3 to 8 and to 33 days, a significant increase in sustainable flux was observed (Chang and Lee, 1998). The reduced fouling rates associated with a decrease in sludge production rates at longer sludge ages, is usually attributed to lower EPS concentrations in the reactor. In addition, increasing SRT could enhance the development of slow growing microorganisms that are able to consume polysaccharides and proteins as substrates and produce less biopolymers (Masse et al., 2006). Overall, it is likely that there is an optimal SRT, between the high fouling tendency at very low SRT and the high viscosity of mixed liquor at very long SRT.

EPS play a major role in the cohesion of the sludge flocs in the MBR as well as the cohesion of the biofilm layers located on carriers in the HG-MBR systems. EPS are also in charge of biofilms viscoelastic properties which in turn, can strongly affect the microbial flocs and biofouling layer resistance to shear. Eventually, EPS are recognized as the most direct and significant factor affecting biofouling in MBRs (Laspidou and Rittmann, 2002; Le-Clech et al., 2006). Soluble EPS in the MLSS was reported as an important factor influencing membrane fouling. A high concentration of soluble EPS was shown to boost membrane fouling tendency (Kimura et al., 2005). Ouyang and Liu (2009) showed that soluble EPS concentration increased at shorter SRT, in which total protein concentrations was higher than polysaccharides in the MLSS supernatant, whereas the total polysaccharide content was higher than the protein in the flocs attached to the membrane surface causing a significant fouling. By increasing the SRT, soluble EPS content was decreased on the membrane surface and membrane filtration resistance was reduced (Ouyang and Liu, 2009). EPS production and accumulation on the UF membranes in MBR systems is a complex process influenced by several factors like the substrate composition, mechanical stress, organic loading rate, MLSS concentration, presence of soluble EPS compounds and membrane properties (Chang and Lee, 1998; Rojas et al. 2005; Rosenberger and Kraume, 2003). Since it would be hard to point out how a combination of so many parameters may influence the properties of the

accumulated on the membrane, direct membrane autopsy and analysis of the accumulated EPS can help to relate between EPS properties and membrane fouling.

In this study, we hypothesized that membrane filterability is strongly influenced by EPS cohesion and viscoelastic properties, important properties of the EPS produced at different sludge removal rates in the MBR (Ng et al., 2006; Ying et al., 2009). Different EPS originated from the membrane at different sludge removal rates showed different adherence and viscoelastic properties that were correlated to the EPS composition and to the fouling rate of the membrane. It was intriguing to see how EPS adherence and viscoelasticity change in correlation to different conditions that promote biofouling to different degree. We also suggest a novel parameter in fouling phenomena of membranes in general, first to be applied to UF membranes, in this study – the ***fluidity*** of the adsorbed EPS layer. This parameter is frequently used to describe biopolymer layers in order to estimate their viscoelasticy (deKerchove and Elimelech, 2006; Feiler et al., 2007). The working objective of this study focused on defining if the EPS accumulated on the UF membrane is more fluidic or more rigid under conditions that promote biofouling.

To study the adherence and viscoelastic properties of the EPS, we utilized a quartz crystal microbalance with dissipation monitoring (QCM-D) technology. QCM-D provides real-time, label free measurements of molecular adsorption and/or interactions taking place on various surfaces (Eydelnant and Tufenkji, 2008; Wang et al., 2007). In addition to assessing adsorbed mass (ng/cm^2 sensitivity), measured as changes in oscillating frequency (F) of the quartz crystal, the energy dissipation (D), which is the reduced energy per oscillation cycle provides novel insights regarding structural properties of adsorbed layers (Nguyen and Elimelech, 2007; Voinova et al., 1999). EPS originated from the UF membrane at different sludge removal rates during the MBR operation was extracted and analyzed. Furthermore, confocal laser scanning microscopy (CLSM) of the biofilm on the UF membrane and EPS composition results were correlated to fouling rate of the UF membrane and to the EPS cohesion and viscoelastic properties.

2. Materials and methods

2.1. HG-MBR system and operating conditions

The HG-MBR was equipped with an immersed UF membrane module of ZeeWeed® (ZW-10) (Zenon Environmental Inc, Canada). The membrane module was made of hollow fibers of polyvinylidene fluoride (PVDF) with a mean pore size of 0.04 μm and a total effective filtering surface area of 0.93 m^2 allowing the removal of pathogens and organic matter. The volume of the bioreactor process tank was 190 L and included activated sludge, AqWise carriers (AqWise, Israel), and the membrane module. AqWise carriers were filled as biofilm support with a filling ratio (carrier volume/reactor volume) of 50% (13.64 kg). The carriers are made from high-density (0.96 g/cm3) polyethylene with diameter and height of 13 mm and a specific surface area of 600 m^2/m^3. The carriers' circulation was driven by an air diffuser. The membrane module was surrounded by an 8 mm mesh for avoiding damage from the moving carriers. The system operated under constant-flux mode with a mode of 5 min filtration and 15 s backwash. A feed domestic sewage mixed with chickens' manure was injected into the bioreactor that was operated under desert ambient conditions. Membrane cleaning was maintained by soaking the membrane module in 750 mg/L sodium hypochlorite supplemented with 250 mg/L sodium dodecyl sulfate (SDS) solution for 16 h, repeatedly for 4 times after each experiment, until the membrane permeability was recovered. Aeration was done through an air diffuser installed directly beneath the membrane module for supplementing oxygen to microorganisms, mixing the liquor and cleaning the membrane with aeration rate of 2.3 m^3/h. Airflow rate was controlled by a rotameter, filtration flux of permeate was monitored volumetrically and TMP was monitored by a digital pressure indicator. The mixed liquor temperature was monitored by a temperature indicator located in the reactor MLSS. The dissolved oxygen (DO) concentration is the mean of the upper, middle and bottom locations in the bioreactor vessel (Model 550, YSI, USA). The bioreactor was employed with a water level sensor was used to keep a constant liquid level in the bioreactor. The HG-MBR was operated over a period of two months at sludge removal rate values of 2, 5, 10, and 30 days. The hydraulic retention times (HRT) of this HG-MBR was 5.5 h for all the experiments. Operating conditions of the HG-MBR at different sludge removal rates are listed in Table 1. The influent and effluent characteristics of the HG-MBR operated at different sludge removal rates are listed in Table 2. As expected, at different sludge removal rates, biomass concentration varies. The suspended and attached biomass concentrations versus time at different sludge removal rates are presented in the supporting information section (Figure S1). By reducing the suspended sludge age, an increased washout of the suspended biomass was observed: The MLSS concentration was lower at shorter sludge removal rates. The mean MLSS concentrations were 4055, 2686, 1678 and 1392 mg/L for the sludge removal rates of 30, 10, 5 and 3 days, respectively (Table 1). Interestingly, the attached biofilm concentration was also reduced. In a similar trend of the decline in MLSS concentration, the decline of the attached biofilm concentration was also observed (Figure S1). The sludge removal rate calculation is taking into account that there was no biomass lost in the effluent of the MBR during its entire operational period. Therefore, the biomass concentration in both the reactor and in the removed sludge stream is the same. SRT, was calculated following Li et al. (1984), $SRT = V \cdot X_V / V_{WS} \cdot \Delta X_V$ The reactor volume was 190 L multiplied by the volumetric fraction occupied by the biofilm's carriers (50%). *V* is the reactor volume occupied by MLSS (L), *VWS*is the flow rate of the removed sludge per day (L day^{-1}), *XV* is the MLSS concentration and Δ*XV* is the MLSS concentration in the removed sludge per day. Since in this work, $XV = \Delta XV$, the suspended sludge retention time is the reactor volume (L) divided by sludge removal rate (L day^{-1}), *V*/*VWS*.

2.2. EPS extraction and analysis

EPS extraction was performed from a single hollow fiber that was cut from the ZW-10 module at the end of every

Table 1 – Operating conditions of the HG-MBR at different removal rates (L day^{-1}) of MLSS.

Parameter	5.9°L day^{-1}	17.7°L day^{-1}	35.5°L day^{-1}	59°L day^{-1}
Estimated SRT (days)	30	10	5	3
Temperature	15.5 ~ 29.4 °C (mean 22.3 °C)	22.2 ~ 28.9 °C (mean 26.3 °C)	20.0 ~ 30.6 °C (mean 28.5 °C)	25.5 ~ 29.4 °C (mean 28.0 °C)
Initial membrane permeability (L/(m^2.hr.bar)) at 20 °C	631.1	465.5	449.8	527.7
Initial membrane resistance (m^{-1})	0.56×10^{12}	0.76×10^{12}	0.79×10^{12}	0.67×10^{12}
Filtrate flux (L/(m^2 h))	44.5 to 38.9	44.8 to 40.6	45.2 to 38.58	45.2 to 37.7
Aeration rate (m^3/hr)	2.3	2.3	2.3	2.3
Hydraulic retention time (hours)	5.1 ~ 5.8	5.0 ~ 5.5	5.0 ~ 5.9	5.0 ~ 6.0
pH in the reactor	6.6 ~ 7.8	6.2 ~ 6.9	6.6 ~ 6.9	6.7 ~ 7.1
Dissolved oxygen, mg O_2/L	0.31 ~ 6.5 (mean 2.6)	0.7 ~ 5.6 (mean 2.8)	0.25 ~ 3.66 (mean 0.89)	2.4 ~ 6.2 (mean 4.3)
MLSS range (mg/L)	2440 to 4580 (mean 4055)	1000 to 3520 (mean 2686)	1225 to 2110 (mean 1678)	1170 to 1575 (mean 1392)
AqWise carriers in the reactor	13.64 kg carriers in the reactor with a bulk filling ratio of 50%			
Operating time (days)	34	26	16	9

experiment. The EPS extraction step was carried out according to Liu and Fang (Liu and Fang, 2002). A 10 cm piece of the fiber was cut and the ends of the fibers attached to the module were sealed. Briefly, the fiber was suspended into 10 mL of 0.1 M NaCl solution in a 50 mL polypropylene tube, and vortexed for 45 min to make sure that the biofilm is totally suspended. Then, 60 μL of 35% formaldehyde (Sigma–Aldrich, Israel) were added to the solution and incubated 1 h in a Vortex Genie 2® (Scientific Industries, USA) at a minimum mixing setting and 4 °C, followed by the addition of 4 mL 1 M sodium hydroxide at 4 °C for 3 h incubation period in order to facilitate dissociation of the acidic groups from the EPS to the solution. Thereafter, the suspension was centrifuged (35,000 rpm, 30 min, 4 °C), the supernatant was filtered through a 0.2 μm hydrophilic nylon filter (Millipore Co.), and dialyzed through a dialysis membrane of 3500 Da (Spectra/Por) for a few days until salts were completely removed. Then the extracted EPS was a lyophilized (FreeZone 2.5 plus) at −80 °C and 0.01 mbar for 48 h. The frozen and dried EPS samples were re-dissolved in 10 mL of double distilled water (DDW) for the determination of dissolved organic carbon (DOC), proteins, and polysaccharides concentrations.

Extracellular protein of the extracted EPS was analyzed using the colorimetric quantitative protein determination with the Bio-Rad© Protein Assay according to Bradford (Bradford, 1977). Polysaccharides contents were determined according to Dubois et al. (DuBois et al., 1956), using glucose and alginic acid as standards. EPS extracted was expressed as DOC concentration measured by using an Apollo 9000 TOC Analyzer (Teledyne Tekmar, United States).

2.3. *Adherence and viscoelastic properties analysis with QCM-D*

EPS was extracted from the UF membrane surface after operating the HG-MBR under different conditions, i.e., at different sludge removal rates of 59, 35.4, 17.7, and 5.9 L day^{-1} (correspond to calculated SRT of 3, 5, 10, and 30 days). The adherence and adsorption kinetics of the EPS was carried out in a QCM-D (Q-Sense AB, Gothenburg, SWEDEN). The QCM-D measurements were performed with AT-cut quartz crystals mounted in an E1 system (Q-sense AB, Gothenburg, SWEDEN). The gold coated crystals with a fundamental resonant frequency of around 5 MHz were coated with Polyvinylidene Fluoride (PVDF) batch number (QSX999, Q-sense). Before each measurement, the crystals were soaked in a 5 mM ethylenediaminetetraacetic acid (EDTA) solution for 30 min, rinsed thoroughly with DDW and dried with pure N_2 gas. The EPS was used in several adsorption measurements to the QCM-D PVDF coated gold sensor. EPS adsorption to the sensor surface is characterized by the change of the oscillation frequency of the PVDF coated gold sensor during parallel flow of aqueous media with flow rate of 150 μl/min above the sensor surface. The variations of frequency, f (Hz) and dissipation factor, D were measured for the three overtones ($n =$, 5, 7, and 9). The working stages for applying aqueous media to the QCM-D flow cell include 5 stages of 20 min each at constant temperature (22 °C). The stages include the following fluids being injected to the QCM-D flow cell: DDW, 10 mM NaCl aqueous solution, 20 mg/L of EPS as DOC (from membrane after MBR operation at different sludge removal rates) dissolved in 10 mM NaCl, 10 mM NaCl aqueous solution, and DDW. The QCM-D results from these experiments were further modeled in which the thickness, shear modulus, and shear viscosity values of the adsorbed EPS layers on the PVDF crystal were calculated. The viscoelastic properties of the EPS layers were calculated based on the Voigt model according to Voinova et al. (Voinova et al., 1999). The density and viscosity of the solution used in this model were 1 g/cm^3 and 10^{-3} Pa s, respectively. The density of the adsorbed layer was fixed at 1.030 g/cm^3, following the recommendations of Gurdak et al. (2005). The best fitting values of the shear viscosity (η), shear modulus (μ), and thickness of the adsorbed layer were obtained by modeling the experimental data of f and D for three overtones using the program Q-Tools provided by Q-Sense AB.

2.4. *CLSM analysis*

At the end of every experiment in which different sludge removal rates were applied in the HG-MBR operation, membrane autopsies were carefully cut to pieces of around

Table 2 – The influent and effluent characteristics of the HG-MBR operated at different removal rates (L day^{-1}) of MLSS.

Parameter	5.9 L day^{-1} (estimated SRT = 30 days)			17.7 L day^{-1} (estimated SRT = 10 days)			59 L day^{-1} (estimated SRT = 3 days)			35.5 L day^{-1} (estimated SRT = 5 days)		
	Influent	Effluent	Percent removal	Influent	Effluent	Percent Removal	Influent	Effluent	Percent Removal	Influent	Effluent	Percent removal
COD, mg/L	418 ± 123	36 ± 13	91.4	529 ± 205	37 ± 18	93.1	483 ± 140	42 ± 25	91.3	495 ± 50	51 ± 18	89.8
BOD, mg/L	171 ± 45	1.3 ± 0.4	99.2	231 ± 60	1.1 ± 0.5	99.5	229 ± 63	1.2 ± 0.4	99.5	317 ± 67	1.5 ± 0.3	99.5
NH_4^+–N, mg/L	30 ± 6.8	1.4 ± 2.8	95.4	38 ± 16	0.1 ± 0.2	99.8	38 ± 5.7	0.3 ± 0.2	99.1	38 ± 4.6	0.9 ± 1.1	97.7
TN, mg/L	35 ± 8.1	24 ± 7.4	31.2	49 ± 12	37 ± 6.3	24.4	46 ± 6.3	31 ± 3.3	33.0	41.9 ± 15	34.6 ± 4.8	17.4
PO_4^{-3}–P, mg/L	10 ± 4.2	7.6 ± 3.3	25.0	14 ± 6.8	12 ± 4.4	15.2	12 ± 3.6	8.4 ± 2.2	29.9	18.6 ± 11.4	16.2 ± 11.3	12.9
TSS, mg/L	171 ± 63	0.2 ± 0.5	99.9	176 ± 97	0.8 ± 1.0	99.5	176 ± 70	0.8 ± 1.1	99.5	269 ± 105	1.0 ± 1.2	99.6
Turbidity, NTU	231 ± 79	0.2 ± 0.1	99.9	245 ± 186	0.3 ± 0.1	99.9	201 ± 85	0.3 ± 0.3	99.8	330 ± 186	0.3 ± 0.1	100.0
EC, mS/cm	1.3 ± 0.2	1.2 ± 0.2	–	1.2 ± 0.1	1.1 ± 0.1	–	1.3 ± 0.2	1.1 ± 0.1	–	1.3 ± 0.1	1.1 ± 0.1	–
pH	7.5 ± 0.3	7.5 ± 0.4	–	7.3 ± 0.2	6.7 ± 0.4	–	7.5 ± 0.2	7.2 ± 0.3	–	7.0 ± 0.2	7.4 ± 0.1	–

1 cm length from the fiber that was cut for the EPS extraction. The membrane pieces were double stained with concanavalin A (ConA) conjugated to Alexa fluor 633, and SYTO9 for probing EPS or microorganisms, respectively. Microscopic observation and image acquisition were performed using Zeiss-Meta 510, a CLSM equipped with Zeiss dry objective LCI Plan-NeoFluar (25 × magnification and numerical aperture of 0.8). The CLSM was equipped with detectors and filter sets for monitoring SYTO9 stained cells and Alexa fluor 633 dye (excitation wavelengths of 488 and 633 nm, respectively). CLSM images were generated using the Zeiss LSM Image Browser. Gray scale images were analyzed, and the specific biovolume ($\mu m^3/\mu m^2$) in the biofouling layer was determined by COMSTAT image-processing software (Heydorn et al., 2000b). For every sample between 4 and 6 positions on the membrane were chosen and microscopically observed, acquired, and analyzed. The ConA, conjugated to Alexa fluor 633 (Invitrogen Co.), was used as a probe to determine the presence of EPS.Briefly, frozen (−20 °C) 100 μL aliquots of 1 mg/mL labeled ConA stock solution were thawed and diluted in 10 mM phosphate buffer (pH 7.5) to 100 μg/mL prior to use in 10 mM phosphate buffer (pH 7.5). An excess electrolyte solution was carefully drawn off from the fouled membrane by gently touching the edge of the specimens with an adsorbing paper (Kimwipes). Then, 100 μL of ConA staining solution were added to cover the samples, which were then incubated in the dark at room temperature for 20 min. Unbound ConA was drawn off the specimens using a three-step wash of 10 mM phosphate buffer. The unbound ConA solution and the washing solutions were carefully removed by gently touching the edge of the specimen with an adsorbing paper. CYTO9 was used for probing the microorganisms in the fouling layer. Excess electrolyte solution was carefully drawn off from a piece of a fouled membrane in the same manner used for ConA staining. Then, 5 μM SYTO9 solution (prepared in 10 mM phosphate buffer, pH 7.5) was added to cover the samples, which were then incubated in the dark at room temperature for 20 min. Excess SYTO9 solution was carefully drawn off with an adsorbing paper. The excess SYTO9 nucleic acid stain that did not bind to the samples was then removed by rinsing three times with a 10 mM phosphate buffer at pH 7.5.

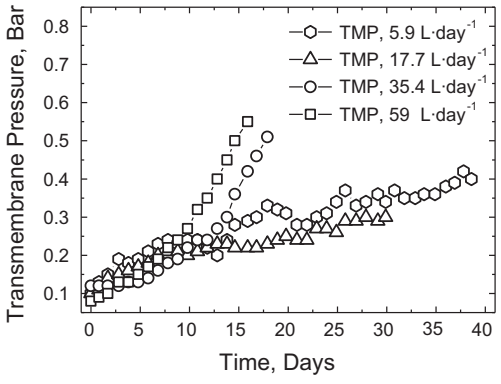

Fig. 1 – The effect of different sludge removal rates (L day^{-1}) on the UF membrane TMP (Bar).

3. Results and discussion

3.1. The effect of sludge removal rate on the filtration performance of the MBR

Fig. 1 shows the variations of TMP over time at the various sludge removal rates. At sludge removal rate of 5.9 and 17.7 L day^{-1} (estimated SRT of 10 and 30 days), the TMP increased slowly, displaying a linear tendency with the increasing TMP rate of 0.0055 and 0.0064 bar per day, respectively. It seems that at sludge removal rate of 17.7 L day^{-1} (estimated SRT of 10 days), the system has the lowest fouling rate. When sludge removal rate was changed to 59 L·day^{-1} (estimated SRT of 3 days), a very sharp increase of TMP from 0.08 to 0.55 bar was observed after 13 days, with an increase rate of 0.027 bar/day, while at sludge removal rate of 35.5 L day^{-1} (estimated SRT of 5 days), an increase rate of 0.016 bar/day was observed. In other words, the fouling rate at sludge removal rate of 59 L day^{-1} (estimated SRT of 3 days) is nearly 5 times higher than that of sludge removal rate of 17.7 L day^{-1} (estimated SRT of 10 days). The extent of fouling is likely to vary according to the MLSS composition including EPS and SMP in the bioreactor that interact with the membrane surface and pores (Chang et al., 2002; Drews, 2010). Therefore, we decided to analyze and compare the adherence and viscoelastic properties of EPS deposited on the membrane. EPS extracted from the membrane operated in the MBR at different SRTs was used for adsorption experiments to a PVDF coated sensors in the QCM-D as well as fouling experiments of single fiber UF membrane unit.

3.2. The effect of sludge removal rate on EPS adherence and viscoelastic properties

In this part of the study, EPS adherence and viscoelastic properties were analyzed by conducting EPS adsorption experiments to PVDF coated sensors in a QCM-D flow cell (Kwon et al., 2006; Li and Wang, 2006; Voinova et al., 1999). As a proof of concept, we used PVDF coated crystals as a model that mimics membrane surface as a substratum for EPS to delineate their adherence and viscoelastic characteristics. EPS were extracted from the membrane surface at the end of each of the fouling experiments (estimated SRT of 3, 5, 10 and 30 days). The final EPS solution was set to 20 mg DOC per liter. Fig. 2(A–B) describes the decrease in frequency and increase in dissipation energy of the PVDF crystal due to adsorption of EPS originated from the membrane taken from the MBR operated at different sludge removal rates. It should be mentioned that EPS measurements with QCM-D are from EPS that was reconstituted on the QCM-D sensor and due to the methodology, physical characteristics of the EPS might be different compare to the EPS on the membrane. Interestingly, the results were very consistent with the effect of sludge removal rate on membrane performance (Fig. 1). The highest EPS adsorption rate expressed as a decrease in the crystal frequency was observed for the EPS extracted from the membrane fiber surface at sludge removal rate of 59 L day^{-1} (estimated SRT of 3 days) while the lowest EPS adsorption rate was observed for the EPS originated from MBR operation at sludge removal rate of 17.7 L day^{-1} (estimated SRT of 10 days).

The simultaneous measurements of the change in frequency Δf are associated with changes in adsorbed mass per area according to the Sauerbrey relation: $\Delta m = -C/n\Delta f$, where Δm is the mass adsorbed to the sensor, n is the overtone number ($n = 1, 3, \ldots$), and C is the mass sensitivity constant of the crystal ($C = 17.7$ ng Hz^{-1} cm^{-2} for a 5 MHz quartz crystal). This relation holds for sufficiently thin, rigid, and non-dissipative film with very limited viscoelastic behavior. Biofilm in general, and EPS layers in particular, are not rigid and they undergo deformation under shear oscillatory motion. In this case, the fluidity of the film can be inferred from the dissipation of the crystal oscillation. The dissipation factor, D, is defined as the ratio of the dissipated and stored energies according to the following: $D = E_{dissipated}/2\pi E_{stored}$.

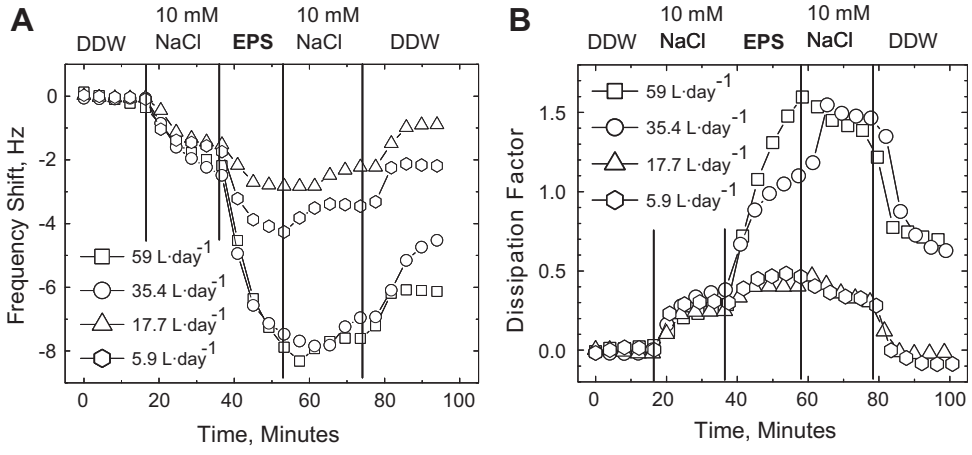

Fig. 2 – EPS adherence properties, extracted from the UF membrane, after runs operated at different sludge removal rates (L day^{-1}): Frequency shifts (A) and dissipation factors (B) during EPS adsorption to PVDF coated QCM-D sensors. A background solution of 10 mM NaCl and ambient pH of 6.2 supplemented with EPS at 20 mg DOC/L was injected to an E1 QCM-D parallel flow cell (Q-Sense, SWEDEN) at a flow rate of 150 μL/min.

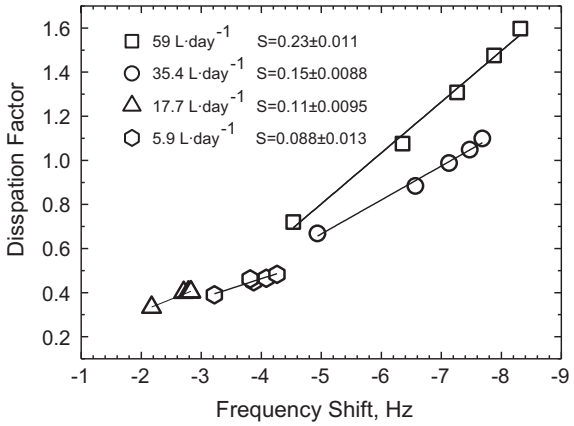

Fig. 3 – Comparison of the fluidity of different EPS, extracted from the UF membrane, after runs operated at different sludge removal rates (L day^{-1}): Dissipation factors versus frequency shifts during adsorption. Slope of the linear regression for the different plots is presented as S, indicating the relative fluidity/rigidity of the EPS layer at each condition (smaller slope relates to higher rigidity of the layer). An ionic strength of 10 mM was adjusted with NaCl at an ambient pH of 6.2 ± 0.1.

The shifts in dissipation (*D*) associated with the decreased frequency (*F*) during EPS adsorption to the PVDF coated sensor are presented in Fig. 2B. Fig. 2B shows representative dissipation shifts obtained during adsorption of EPS extracted from the membrane originated from the MBR operated at different sludge removal rate conditions. As previously reported, the slope of ΔD over ΔF gives the magnitude of the variations in the adsorbed layer fluidity, the main factor in charge of damping the quartz vibration (Notley et al., 2005; Schofield et al., 2007). This ΔD over ΔF shows the induced energy dissipation per coupled unit mass, eliminating time as an explicit parameter, and making it possible to analyze the effects of EPS adsorption on the damping of the crystals' resonance frequency.

The fluidic properties of the EPS layer on the crystal are determined by studying this relationship, between the shifts in dissipation (*D*) and the shifts in frequency (*F*) obtained by the QCM-D (Fig. 2). Harmonic 7 (35 MHz) was used for this relation. For each of the sludge removal rate conditions, a linear relationship was observed between *D* and *F* during the EPS adsorption onto the crystal surface. Each linear correlation corresponds to the EPS adsorption stage after acquiring a baseline with the background solution of 10 mM NaCl. The slopes of the linear relationship between *D* and *F* for each of the HG-MBR operational conditions are shown in Fig. 3. The trends observed for the change in slopes show an interesting behavior in which at higher sludge removal rate of 35.5 and 59 L day^{-1} (estimated SRT of 5 and 3 days, respectively), the extracted EPS layers are more fluid compared to the EPS layers extracted from the membrane exposed to slower sludge removal rates of 5.9 and 17.7 L day^{-1} (estimated SRT of 30 and 10 days, respectively). It seems that in addition to a higher EPS adherence (Fig. 2A), fluidity of the fouling layer is likely playing an important role in its accessibility to the membrane pores that eventually are being accumulated more rapidly by the EPS extracted at a faster sludge removal rate (estimated SRT of 5 and 3 days). Recently, using similar UF membrane, we have shown that EPS fluidity and swelling induced at high pH, have major contribution to pore clogging (Sweity et al., 2011).

The fitted values of the elastic shear modulus and shear viscosity of the adsorbed EPS layers were calculated using the Voigt model (Voinova et al., 1999, Q-Tools software of the QCM-D). The fitted values further confirmed the results showing higher fluidity of EPS extracted from the faster fouled membrane. The variations in these two parameters are calculated for each EPS obtained from the membrane under different conditions of sludge removal rate and are shown in Table 3. It is shown in Table 3 that for the slower sludge removal rate of 5.9 and 17.7 L day^{-1} (estimated SRT 30 and 10 days), the EPS is much more viscoelastic. An ambitious study would be to find the operational conditions that induce such characters of the EPS that eventually deposits on the UF membranes. As already mentioned, the way soluble EPS is produced and deposited on the UF membrane is a complex process affected by many parameters. Possible reasons for the differences in the adherence and viscoelasticity of the EPS originated from the membrane can be differences in the biomass concentration in the HG-MBR (Supporting information – Figure S1), feed to biomass (F/M) ratio (Supporting information – Figure S2) as well as different levels of proteins and polysaccharides in EPS at different locations in the HG-MBR (Supporting information – Figure S3). In conclusion, EPS extracted from the membrane operated at lower sludge removal rate (longer estimated SRT) was more viscoelastic with more rigid conformation analyzed in the QCM-D, while in contrast, a higher fluidity was detected for EPS extracted from the membrane operated at faster sludge removal rates (shorter estimated SRT) (Table 1 and Fig. 3).

Table 3 – Thickness, shear modulus, and viscosity of the deposited EPS layers extracted from the HG-MBR at different removal rates (L day^{-1}) of MLSS (presented in duplicate).

	59 L day^{-1} (estimated SRT = 3 days)		35.5 L day^{-1} (estimated SRT = 5 days)		17.7 L day^{-1} (estimated SRT = 10 days)		5.9 L day^{-1} (estimated SRT = 30 days)	
Thickness, nm	2.8	2.4	3.5	2.6	2.2	2.8	3.3	2.8
Viscosity, kg m^{-1} s^{-1}	0.0010	0.0012	0.0011	0.0011	0.0015	0.0018	0.0018	0.0018
Shear modulus, Pa	$2.6\cdot10^4$	$3.2\cdot10^4$	$6.4\cdot10^4$	$4.5\cdot10^4$	$1.5\cdot10^5$	$1.5\cdot10^5$	$2.1\cdot10^5$	$4.5\cdot10^5$

3.3. The relation between EPS composition, adherence, and membrane fouling rate

To further study EPS adherence and accumulation on the membrane, filtration of the extracted EPS from the membrane of the MBR was performed through a single UF fiber under representative ionic strength of 10 mM with and without 0.5 mM of calcium cations (Sweity et al., 2011). Hence, faster decline in membrane permeability was observed for EPS originated at higher sludge removal rate of 59 L day^{-1} (estimated SRT of 2 days) under both conditions (Fig. 4A and B). The slowest decline in membrane permeability was observed for sludge removal rates of 17.7 and 5.9 L day^{-1} (estimated SRT of 10 and 30 days), with and without calcium (Fig. 4A and B). EPS composition and amount per membrane surface area was quantified and related to the membrane fouling rate in the HG-MBR and in the single fiber filtration unit as well as to the QCM-D analysis. For EPS extraction and analysis, one fiber was cut from the membrane module at the end of each experiment operated at a constant sludge removal rate. Fig. 5 presents the EPS (as DOC content), proteins, and polysaccharides accumulation on the membrane surface (μg/cm^2) of the HG-MBR at the different sludge removal rates. The results show that the highest EPS accumulation on the membrane of the HG-MBR occurred at a sludge removal rate of 59 L day^{-1} (estimated SRT of 3 days), followed, in turn, during MBR operation at sludge removal rates of 35.5, 5.9 and 17.7 L day^{-1} (estimated SRT of 5, 30 and 10 days, respectively). The protein accumulation at the estimated SRT of 10, 5 and 3 days was very similar and at a relatively low level (Fig. 5). However, the accumulation of polysaccharides on the membrane surface exhibited a different behavior in contrast to the proteins, in which an extremely high level of polysaccharide accumulation was observed for the highest sludge removal rate of 59 L day^{-1} (estimated SRT of 3 days), while at sludge removal rate of 17.7 L day^{-1} (estimated SRT of 10 days), the lowest accumulation was obtained (Fig. 5). Combining the results so far, at the highest removal rate of sludge, polysaccharides content in EPS is elevated on the membrane (Fig. 5) and in general, per biomass unit (VSS), also in other locations in the HG-MBR (Figure S4). The increased polysaccharides content on the membrane is proposed to be a result of stronger adherence properties of the EPS. This stronger adhesion of EPS, eventually reduce membrane permeability observed in Fig. 4 and most likely increase the rate of TMP elevation (bar/day) in the MBR (Fig. 1).

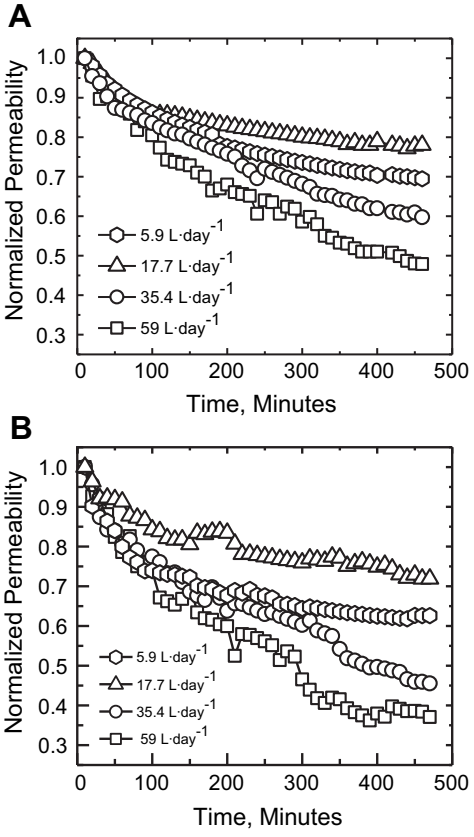

Fig. 4 – Normalized permeability during fouling of a single fiber UF membrane with EPS extracted from the HG-MBR-UF membrane at the end of runs operated at different sludge removal rates (L day^{-1}). Fouling experiments were carried out at ionic strength of 10 mM (adjusted with NaCl) with (A) and without (B) 0.5 mM calcium cations. The pressure was set at all experiments between 0.14 and 0.18 bar. Initial permeability of the UF PVDF fibers (Zenon, GE) was 0.15 ± 0.02 cm·min^{-1}·bar^{-1}.

It is generally accepted that polysaccharides can mediate cohesion of cells, and play an important part in maintaining the structural integrity of biofilms (Christensen, 1989; Liu and Tay, 2001; Ross, 1984). Polysaccharides can mediate cell-to-cell interaction in two ways: firstly, polysaccharides bridge cells to form a three-dimensional structure, which may then interact with more bacterial cells and particulate matter (Ross, 1984); secondly, dispersed bacteria are negatively charged at usual pH values, and electrostatic repulsion exists between cells. It had been proposed that extracellular polymers could change the surface negative charge of bacteria, and thereby bridge two neighboring bacterial cells physically to each other as well as other inert particulate matter (Schmidt and Ahring, 1994; Shen et al., 1993). In this study, the higher polysaccharides content in EPS extracted at the fastest sludge removal rate (estimated SRT of 3 days) showed the strongest adherence as

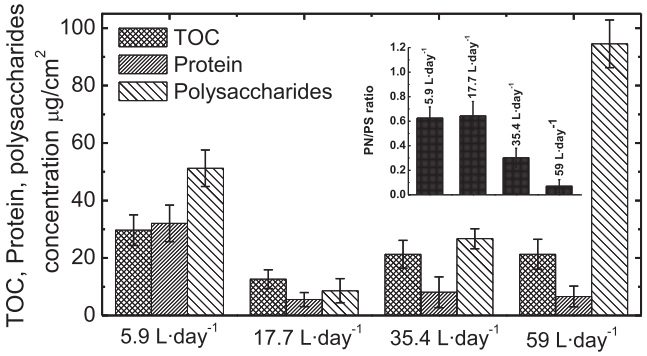

Fig. 5 – The concentrations of accumulated components of EPS presented as TOC, proteins, and polysaccharides on the membrane surface. Inserted figure shows protein/polysaccharide ratio of EPS components on the membrane surface.

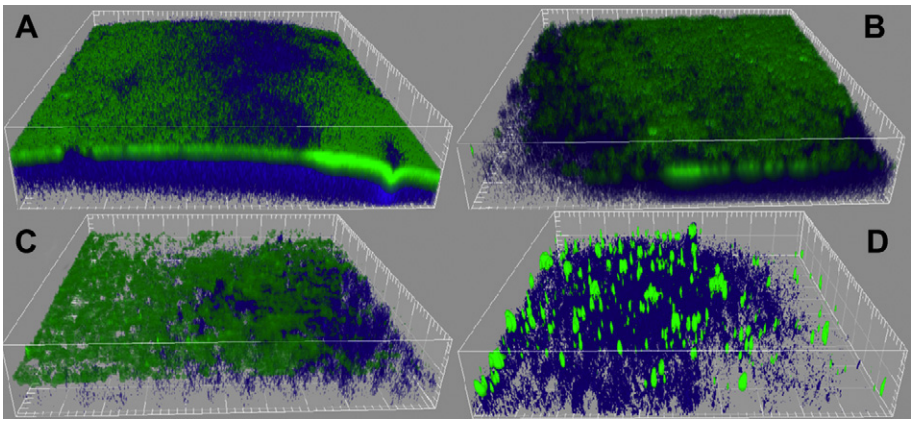

Fig. 6 – CLSM analysis of the biofouling layer on the membrane surface at the end of runs operated at different sludge removal rates (L day^{-1}). Sludge removal rates are (A) 59 L day^{-1}; (B) 35.4 L day^{-1}; (C) 17.7 L day^{-1}; and (D) 5.9 L day^{-1}. Blue and green spots represent extracellular polysaccharides and microorganisms, respectively. Total biomass of EPS and cells is expressed as specific biovolume ($\mu m^3/\mu m^2$) as analyzed with COMSTAT biofilm software: (A) 95.8 ± 25.2; (B) 45.4 ± 10.1; (C); 31.1 ± 13.2 and (D) 57.2 ± 22.2 for EPS and (A) 28.5 ± 5.1; (B) 24.3 ± 3.6; (C) 6 ± 3.5; and (D) 13.1 ± 2.71 for viable cells. (For interpretation of the references to color in this figure legend, the reader is referred to the web version of this article.)

analyzed in the QCM-D and led to a greater loss of filterability in the single UF fiber unit (Figs. 2 and 4). Other studies also correlated between polysaccharides concentration and membrane fouling rate in MBR systems (Rosenberger et al., 2006; Fan et al., 2006). Interestingly, a higher fluidity of the EPS adsorbed layer was observed for the EPS extracted from the membrane at the faster sludge removal rate of 59 and 35.5 L day^{-1} (estimated SRT of 3 and 5 days). The higher fluidity of EPS is likely a part of increased accessibility of the EPS to the membrane pores that eventually increase its concentration within the membrane (Fig. 5).

EPS adherence properties are primarily affected by polysaccharides (Herzberg et al., 2009a,b) and corroborated with PN/PS ratios analyzed in the EPS extracted from the membrane at different sludge removal rates (Fig. 5, inserted graph): Lower PN/PS ratio correlates well with the higher adherence of the EPS observed by the QCM-D (Fig. 2). With regard to the fluidity of the EPS layer, previous results in our lab also showed a decrease in elasticity (lower shear modulus) of EPS due to over-expression of alginate (Results not shown) as well as a relation between increased EPS swelling, fluidity, and reduced UF membrane permeability (Sweity et al., 2011).

3.4. *Variations in biofilm formation on the membrane at different SRTs*

A correlation between a decrease in membrane performance at different sludge removal rates and an increase in the EPS content on the membrane is observed in Figs. 1 and 6. Variations in biofilm formation (amount of EPS and viable cells) were observed on the membrane surface using CLSM imaging (Fig. 6A–D) and analyzed using COMSTAT biofilm software (Heydorn et al., 2002, 2000a). On the membrane surface, at the highest sludge removal rate of 59 L day^{-1} (estimated SRT of 3 days), the highest polysaccharides content was analyzed using the labeled lectin, concanavalin A (Figs. 5 and 6A). The lowest polysaccharides content was observed at sludge removal rate of 17.7 L day^{-1} (estimated SRT of 10 days) (Figs. 5 and 6C). CLSM results also corroborate with the measured fouling rate, in which at a sludge removal rate of 17.7 L day^{-1} (estimated SRT of 10 days), the increase in TMP was the lowest and at sludge removal rate of 59 L day^{-1} (estimated SRT of 3 days), the increase in TMP was the highest.

4. Concluding remarks

In this work, a novel approach of EPS analysis was taken for studying membrane biofouling in HG-MBR system. EPS, originating from a fouled UF membrane was extracted and its adherence and viscoelasticity were determined using QCM-D. EPS was collected from the membrane under different fouling conditions affected by the sludge removal rate from the HG-MBR. The different fouling conditions of the UF membrane were correlated well to EPS adherence, where stronger adhesion of the EPS was observed for EPS extracted from the fouling experiments conducted under conditions of higher sludge removal rate, in which the TMP elevation rate was higher. EPS layer fluidity, a new parameter to be used in membrane fouling phenomena, as well EPS viscoelastic properties can also explain the stronger fouling propensity of EPS extracted from membranes with lower permeability. We propose that the more fluidic the EPS layers are, their accessibility to the membrane pores is higher, where they can penetrate and block the pores. Shear modulus of elasticity and shear viscosity are critical parameters influencing biofilm and EPS cohesion (Ahimou et al., 2007; deKerchove and Elimelech, 2006). These parameters correlate to an improved membrane performance: As the EPS in the membrane is more elastic and viscous, reduced fouling is observed and the ratio of proteins to polysaccharides is higher.

Acknowledgement

This study was supported by USAID Middle East Regional Cooperation (MERC) Program, project number: M29-048.

Appendix. Supplementary material

Supplementary data associated with this article can be found in the online version, at doi:10.1016/j.watres.2011.09.038.

REFERENCES

Ahimou, F., Semmens, M.J., Novak, P.J., Haugstad, G., 2007. Biofilm cohesiveness measurement using a novel atomic force microscopy methodology. Applied and Environmental Microbiology 73, 2897–2904.

Al-Amoudi, A.S., Farooque, A.M., 2005. Performance restoration and autopsy of NF membranes used in seawater pretreatment. Desalination 178, 261–271.

Bradford, M., 1977. A rapid and sensitive method for the quantitation of microgram quantities of protein utilizing the principle of protein dye-binding. Analytical Biochemistry 72, 248–254.

Chang, I.-S., Lee, C.-H., 1998. Membrane filtration characteristics in membrane-coupled activated sludge system – the effect of physiological states of activated sludge on membrane fouling. Desalination 120, 221–233.

Chang, I.S., Le Clech, P., Jefferson, B., Judd, S., 2002. Membrane fouling in membrane bioreactors for wastewater treatment. Journal of Environmental Engineering–ASCE 128, 1018–1029.

Cho, J., Song, K.-G., Ahn, K.-H., 2005a. The activated sludge and microbial substances influences on membrane fouling in submerged membrane bioreactor: unstirred batch cell test. Desalination 183, 425–429.

Cho, J., Song, K.G., Yun, H., Ahn, K.H., Kim, J.Y., Chung, T.H., 2005b. Quantitative analysis of biological effect on membrane fouling in submerged membrane bioreactor. Water Science and Technology 51, 9–18.

Christensen, B.E., 1989. The role of extracellular polysaccharides in biofilms. Journal of Biotechnology 10, 181–201.

Comte, S., Guibaud, G., Baudu, M., 2006. Relations between extraction protocols for activated sludge extracellular polymeric substances (EPS) and EPS complexation properties part I. Comparison of the efficiency of eight EPS extraction methods. Enzyme and Microbial Technology 38, 237–245.

deKerchove, A.J., Elimelech, M., 2006. Structural growth and viscoelastic properties of adsorbed alginate layers in monovalent and divalent salts. Macromolecules 39, 6558–6564.

DuBois, M., Gilles, K.A., Hamilton, J.K., Rebers, P.A., Smith, F., 1956. Colorimetric method for determination of sugars and related substances. Analytical Chemistry 28, 350–356.

Drews, A., 2010. Membrane fouling in membrane bioreactors – characterisation, contradictions, cause and cures. Journal of Membrane Science 363, 1–28.

Eydelnant, I.A., Tufenkji, N., 2008. Cranberry derived proanthocyanidins reduce bacterial adhesion to selected biomaterials. Langmuir 24, 10273–10281.

Fan, F., Zhou, H., Husain, H., 2006. Identification of wastewater sludge characteristics to predict critical flux for membrane bioreactor processes. Water Research 40, 205–212.

Feiler, A.A., Sahlholm, A., Sandberg, T., Caldwell, K.D., 2007. Adsorption and viscoelastic properties of fractionated mucin (BSM) and bovine serum albumin (BSA) studied with quartz crystal microbalance (QCM-D). Journal of Colloid Interface Science 315, 475–481.

Flemming, H.C., Wingender, J., 2001. Relevance of microbial extracellular polymeric substances (EPSs) – part I: structural and ecological aspects. Water Science and Technology 43, 1–8.

Gurdak, E., Dupont-Gillain, C.C., Booth, J., Roberts, C.J., Rouxhet, P. G., 2005. Resolution of the vertical and horizontal heterogeneity of adsorbed collagen layers by combination of QCM-D and AFM. Langmuir 21, 10684–10692.

Han, S.S., Bae, T.H., Jang, G.G., Tak, T.M., 2005. Influence of sludge retention time on membrane fouling and bioactivities in membrane bioreactor system. Process Biochemistry 40, 2393–2400.

Herzberg, M., Kang, S., Elimelech, M., 2009a. Role of extracellular polymeric substances (EPS) in biofouling of reverse osmosis membranes. Environmental Science and Technology 43, 4393–4398.

Herzberg, M., Rezene, T.Z., Ziemba, C., Gillor, O., Mathee, K., 2009b. Impact of higher alginate expression on deposition of Pseudomonas aeruginosa in radial stagnation point flow and reverse osmosis systems. Environmental Science and Technology 43, 7376–7383.

Heydorn, A., Ersboll, B., Kato, J., Hentzer, M., Parsek, M.R., Tolker-Nielsen, T., Givskov, M., Molin, S., 2002. Statistical analysis of pseudomonas aeruginosa biofilm development: impact of mutations in genes involved in twitching motility, cell-to-cell signaling, and stationary-phase sigma factor expression. Applied and Environmental Microbiology 68, 2008–2017.

Heydorn, A., Ersboll, B.K., Hentzer, M., Parsek, M.R., Givskov, M., Molin, S., 2000a. Experimental reproducibility in flow-chamber biofilms. Microbiology-UK 146, 2409–2415.

Heydorn, A., Nielsen, A.T., Hentzer, M., Sternberg, C., Givskov, M., Ersboll, B.K., Molin, S., 2000b. Quantification of biofilm structures by the novel computer program COMSTAT. Microbiology-UK 146, 2395–2407. Uk.

Judd, S., 2006. The MBR Book: Principles and Applications of Membrane Bioreactors in Water and Wastewater Treatment. Elsevier Science, London.

Kimura, K., Yamato, N., Yamamura, H., Watanabe, Y., 2005. Membrane fouling in pilot-scale membrane bioreactors (MBRs) treating municipal wastewater. Environmental Science and Technology 39, 6293–6299.

Kraume, M., Drews, A., 2010. Membrane bioreactors in waste water treatment – status and trends. Chemical Engineering and Technology 33, 1251–1259.

Kwon, K.D., Green, H., Bjoorn, P., Kubicki, J.D., 2006. Model bacterial extracellular polysaccharide adsorption onto silica and alumina: quartz crystal microbalance with dissipation monitoring of dextran adsorption. Environmental Science and Technology 40, 7739–7744.

Laspidou, C.S., Rittmann, B.E., 2002. A unified theory for extracellular polymeric substances, soluble microbial products, and active and inert biomass. Water Research 36, 2711–2720.

Le-Clech, P., Chen, V., Fane, T.A.G., 2006. Fouling in membrane bioreactors used in wastewater treatment. Journal of Membrane Science 284, 17–53.

Lee, W., Kang, S., Shin, H., 2003. Sludge characteristics and their contribution to microfiltration in submerged membrane bioreactors. Journal of Membrane Science 216, 217–227.

Li, A.Y., Kothari, D., Corrado, J.J., 1984. Application of membrane anaerobic reactor system for the treatment of industrial wastewater. In: Proc. 39th Industrial Waste Conf. Purdue Univ., West Lafayette, Indiana, pp. 627–636.

Li, X.Y., Wang, X.M., 2006. Modelling of membrane fouling in a submerged membrane bioreactor. Journal of Membrane Science 278, 151–161.

Liu, H., Fang, H.H.P., 2002. Extraction of extracellular polymeric substances (EPS) of sludges. Journal of Biotechnology 95, 249–256.

Liu, Y., Tay, J.H., 2001. Detachment forces and their influence on the structure and metabolic behaviour of biofilms. World Journal of Microbiology & Biotechnology 17, 111–117.

Masse, A., Sperandio, M., Cabassud, C., 2006. Comparison of sludge characteristics and performance of a submerged membrane bioreactor and an activated sludge process at high solids retention time. Water Research 40, 2405–2415.

Meng, F., Chae, S., Drews, A., Kraume, M., Shin, H., Yang, F., 2009. Recent advances in membrane bioreactors (MBRs): membrane fouling and membrane material. Water Research 43, 1489–1512.

Morgan, J.W., Forster, C.F., Evison, L., 1990. A comparative study of the nature of biopolymers extracted from anaerobic and activated sludges. Water Research 24, 743–750.

Ng, H.Y., Tan, T.W., Ong, S.L., 2006. Membrane fouling of submerged membrane bioreactors: impact of mean cell residence time and the contributing factors. Environmental Science and Technology 40, 2706–2713.

Nguyen, T.H., Elimelech, M., 2007. Adsorption of plasmid DNA to a natural organic matter-coated silica surface: kinetics, conformation, and reversibility. Langmuir 23, 3273–3279.

Notley, S.M., Eriksson, M., Wagberg, L., 2005. Visco-elastic and adhesive properties of adsorbed polyelectrolyte multilayers determined in situ with QCM-D and AFM measurements. Journal of Colloid and Interface Science 292, 29–37.

Nuengjamnong, C., Kweon, J.H., Cho, J., Ahn, K.H., Polprasert, C., 2005. Influence of extracellular polymeric substances on membrane fouling and cleaning in a submerged membrane bioreactor. Colloid Journal 67, 351–356.

Ouyang, K., Liu, J., 2009. Effect of sludge retention time on sludge characteristics and membrane fouling of membrane bioreactor. Journal of Environmental Sciences 21, 1329–1335.

Rojas, M.E.H., Van Kaam, R., Schetrite, S., Albasi, C., 2005. Role and variations of supernatant compounds in submerged membrane bioreactor fouling. Desalination 179, 95–107.

Rosenberger, S., Kraume, M., 2003. Filterability of activated sludge in membrane bioreactors. Desalination 151, 195–200.

Rosenberger, S., Laabs, C., Lesjean, B., Gnirss, R., Amy, G., Jekel, M., Schrotter, J.-C., 2006. Impact of colloidal and soluble organic material on membrane performance in membrane bioreactors for municipal wastewater treatment. Water Research 40, 710–720.

Ross, W.R., 1984. The phenomenon of sludge pelletization in the anaerobic treatment of a maize processing waste. Water SA 10, 197–204.

Schmidt, J.E., Ahring, B.K., 1994. Extracellular polymers in granular sludge from different upflow anaerobic sludge blanket (UASB) reactors. Applied Microbiology and Biotechnology 42, 457–462.

Schofield, A.L., Rudd, T.R., Martin, D.S., Fernig, D.G., Edwards, C., 2007. Real-time monitoring of the development and stability of biofilms of streptococcus mutans using the quartz crystal microbalance with dissipation monitoring. Biosensors and Bioelectronics 23, 407–413.

Shen, C.F., Kosaric, N., Blaszczyk, R., 1993. The effect of selected heavy-metals (Ni, Co and Fe) on anaerobic granules and their extracellular polymeric substance (EPS). Water Research 27, 25–33.

Sombatsompop, K., Visvanathan, C., Ben Aim, R., 2006. Evaluation of biofouling phenomenon in suspended and attached growth membrane bioreactor systems. Desalination 201, 138–149.

Sweity, A., Ying, W., Belfer, S., Oron, G., Herzberg, M., 2011. pH effects on the adherence and fouling propensity of extracellular polymeric substances in a membrane bioreactor. Journal of Membrane Science 378, 186–193.

Trussell, R.S., Merlo, R.P., Hermanowicz, S.W., Jenkins, D., 2006. The effect of organic loading on process performance and membrane fouling in a submerged membrane bioreactor treating municipal wastewater. Water Research 40, 2675–2683.

Voinova, M.V., Rodahl, M., Jonson, M., Kasemo, B., 1999. Viscoelastic acoustic response of layered polymer films at fluid-solid interfaces: continuum mechanics approach. Physica Scripta 59, 391–396.

Wang, X., Ruengruglikit, C., Wang, Y.W., Huang, Q., 2007. Interfacial interactions of pectin with bovine serum albumin studied by quartz crystal microbalance with dissipation monitoring: effect of ionic strength. Journal of Agricultural and Food Chemistry 55, 10425–10431.

Yang, Q., Chen, J., Zhang, F., 2006. Membrane fouling control in a submerged membrane bioreactor with porous, flexible suspended carriers. Desalination 189, 292–302.

Ying, W., Herzberg, M., Yang, F., Bick, A., Oron, G., 2009. Hybrid growth membrane bioreactor (HG-MBR): the indirect impact of sludge retention time on membrane fouling. Desalination and Water Treatment 10, 27–32.